

This is a peer-reviewed preprint submitted to EarthArXiv. The manuscript is part of Chapter 3-2-6 of The Encyclopedia of Volcanoes, 3rd ed. Editors: C. Bonadonna, L. Caricchi, A. Clarke, P. Cole, J. Lindsay, J. Lowenstern, R. Robertson and M. L. Villegas.

PART 3: Volcanic eruptions and associated products

CHAPTER 2.6 : Volcano stratigraphy and mapping

Karen Fontijn^{1*}, Benjamin Bernard², Drew T. Downs³, Judy Fierstein⁴, Guido Giordano⁵, Graham Leonard⁶, Natalia Pardo⁷, Patricia Sruoga⁸, Takehiko Suzuki⁹

¹ Department of Geosciences, Environment and Society, Université libre de Bruxelles, Brussels, Belgium

² Instituto Geofísico de la Escuela Politécnica Nacional, Quito, Ecuador

³ U.S. Geological Survey, Hawaiian Volcano Observatory, Hilo, Hawaii, USA

⁴ U.S. Geological Survey, Volcano Science Center, Moffett Field, California, USA

⁵ Geology Section, Department of Sciences, Università Roma Tre, Rome, Italy

⁶ Earth Structure and Processes Department, GNS Science, New Zealand

⁷ Department of Geosciences, Universidad de los Andes, Bogotá, Colombia

⁸ CONICET-SEGEMAR, Buenos Aires, Argentina

⁹ Department of Geography & Research Center for Hazard Mitigation in Volcanic Islands and Urban Areas, Tokyo Metropolitan University, Japan

*Corresponding author: Karen.Fontijn@ulb.be

Abstract

Volcano-geologic mapping and stratigraphic reconstructions provide important information toward understanding patterns of edifice construction and destruction of volcanic systems, their eruptive histories and recurrence rates, and magmatic evolution and plumbing systems, all of which are required to make informed hazard assessments. Geologic mapping of volcanic terrains also provides context in the search for and identification of natural resources, including geothermal reservoirs and magmatic-related ore deposits, and can provide useful background for communication and outreach. Most volcano-geologic maps and chrono-stratigraphic frameworks are based on a systematic lithostratigraphic approach and are constructed using an iterative process whereby field observations and mapping alternate with acquisition of rock compositional and geochronological data. Modern technological and analytical tools have greatly advanced geochemical and geochronological data acquisition and accuracy, while some technologies have provided new useful tools for fieldwork, including in poorly accessible environments.

Key words

Volcano geology; geologic mapping; eruption history; tephrostratigraphy; volcanic architecture; volcanic successions; volcano tectonics

Introduction

Geologic mapping is essential to understanding Earth's dynamic history. In volcanic terrains, a geologic map is fundamental toward establishing the eruptive history of a whole system and to building a complete time-volume-composition-behavior record that provides the much-needed context for almost all other geological studies of volcanoes. These include petrology and geochemistry for understanding magmatic evolution and plumbing systems [E1], physical volcanology for understanding eruptive and emplacement processes [E2], and distinguishing variable magnitudes, periodicities, and styles of eruption that enhance our understanding of attendant hazards [E3-E4]. A detailed map with a solid chrono-stratigraphic framework provides context for evaluating volcanic and magmatic processes at volcanoes and volcanic fields that change over space and time.

Objectives and use of volcano geologic maps and stratigraphy

A geologic map of a volcano is a graphic representation of a large assemblage of data that includes all that has been learned about its eruptive history. Geologic maps of volcanoes and volcanic fields, combined with robust chrono-stratigraphic frameworks of modern terrains form the basis of key products used in fundamental and applied volcanology research, including at volcano observatories, such as composite lithostratigraphic columns displaying frequency-magnitude relationships of past eruptions and long-term (probabilistic) hazard assessments [E3]. Such assessments ultimately provide inputs for risk assessments and disaster risk reduction [E5]. Ideally, eruption histories from maps and other sources, together with the volcano system models they inform, are used before and during monitoring and crisis response [E6-E7-E8] and serve as a basis for communication and outreach, including communication with the scientific community, government agencies, emergency managers, and/or the general public [E9-E10].

Picturesque landscapes with colorful strata, curious morphologies, and intriguing geologic stories about how and when they formed have led to the establishment of volcano-centered geoheritage sites and increasing volcano tourism (e.g. UNESCO Global Geoparks) [E11-E12]. Such initiatives provide educational opportunities to explain to a broad audience the wider societal benefits of studying volcanoes [E9].

Detailed volcano-structural maps combined with geophysical observations of the shallow subsurface (e.g., resistivity and magneto-telluric surveys) and gas and fluid geochemical analyses (e.g. soil CO₂ flux, fumarole, or hot spring geochemistry) help in building conceptual models of geothermal reservoirs and fluid pathways, and target zones for geothermal exploration and drilling [E13-E14]. In ancient terrains, correct identification of altered volcanogenic deposits might help in assessing potential ore deposits associated with magmatic processes, such as epithermal gold-silver, copper-bearing volcanogenic massive sulfide ores, or diamondiferous kimberlites [E15-E16].

[Additional Reading QR1: "Mapping volcano-related resources"]

Volcanoes are dynamic environments

Volcanic areas are dynamic, whether actively erupting or not. Many geologic processes act on timescales of thousands to millions of years; however, volcanic eruptions and processes can alter landscapes and hydrographic networks over extremely short timeframes (minutes to years). Explosive events can destroy an edifice and, at the same time, provide large amounts of material to surrounding sedimentary environments. Non-eruptive processes such as volcano-edifice collapses can also catastrophically destroy volcanic edifices [E17]. Volcanic deposits can therefore show complex lateral facies variations and contacts at the scale of individual outcrops [1]. Whether by initial emplacement processes or by subsequent reworking, the numerous details of a volcanic history, necessary to provide a sound basis for long-term quantitative hazard assessments, can only be revealed through mapping and stratigraphic reconstruction at adequate spatial and temporal resolutions. A multifaceted approach is therefore needed to produce volcano-geologic maps and to reconstruct volcanic stratigraphy, that include descriptions of each unit, the unit's unique features, and its distribution in the area of interest [1-4].

The progressive and continued development of physical volcanology, and advances in geochronological and geochemical techniques since the 1960s, have generally led to more detailed maps and chrono-stratigraphic reconstructions of volcanic terrains. Modern remote sensing technologies allow for high-resolution digital terrain models, greatly facilitating identification and mapping of large-scale structures and major units that support targeted ground-truthing field campaigns [1, 4].

In this chapter, we introduce the primary methods and approaches used in geologic mapping of volcanoes and stratigraphic reconstruction. We start at the larger scale of the volcano-geologic map, discuss general approaches to fieldwork, and then focus on compiling tephrostratigraphic reconstructions. The mapping and tephrostratigraphy approaches are each illustrated by case studies; together they can be used to reconstruct complete eruptive histories of volcanoes and volcanic fields. We highlight some common challenges and limitations, as well as some recent developments and advances in such field studies.

Methods to carry out volcano stratigraphy and mapping

General principles

Mapping volcanoes and establishing volcanic stratigraphy requires an iterative process. Initial field work that establishes eruptive units distinguished in large part by close examination with a hand lens is corroborated by petrographic, geochemical, paleomagnetic, and geochronologic data, which then inform additional rounds of field and laboratory work. Ultimately, a description of each eruptive unit includes a summary of age, vent site, distribution, lithology, composition, mineralogy, structures, contact relations, and any other characteristics integral to that unit. Compositionally zoned units and evolution of volcanoes through time provide a wealth of eruptive and pre-eruptive information. Additionally, because most volcano contacts are, in some sense, unconformable, much can be learned by scrutinizing the geometry, lithology, and missing time at contacts. Establishing compositional variations, the range of eruptive styles and ages of events contribute to reconstructing the complex interaction between short-lived constructional episodes of edifice growth, when fresh material is deposited at the surface, and longer periods of quiescence during which the edifice and terrain are gradually degraded and deposits

remobilized. Edifice destruction, or remobilization of previously emplaced deposits, may also happen instantaneously pre-, syn-, or post-eruption, due to rapid deposition of newly emplaced units, or to caldera (vertical) or sector (lateral) collapse. These rapid shifts between construction and destruction lead to the formation, and sometimes chaotic stacking, of rock formations that are often delineated by unconformities and abundant reworked intervals (epiclastic deposits), depending on the nature of the erupted material (e.g., loose volcanoclastic debris vs. coherent lava), topography around the volcano, and local climate. **Figure 1** presents a small selection of outcrop-scale photos of a range of volcanic deposits and rocks.

When making initial field observations, use of clear, generic terminology to describe volcanic products is the best way to support later robust interpretations. Avoiding the tendency to prematurely apply genetic terminology based on a limited number of observations will encourage consideration of all observations, and not only those that fit preconceived notions. For detailed guidance on terminology and types of observations necessary to reach an interpretation of volcanic rock and deposit emplacement mechanisms, we refer to [5]. Those authors propose a multi-step iterative procedure that can be applied to any type of volcanic succession, including ancient terrains, and to both coherent rocks (lavas and intrusions) through fragmental and volcanoclastic facies. The procedure includes describing lithological and petrological characteristics, followed by describing outcrop- or drill core-scale depositional and emplacement features, which together lead to a genetic deposit name [5].

[Additional Reading QR2: “Volcano-geologic mapping and facies descriptions”]

In the following sections we provide an overview of some practical aspects of making volcano-geologic maps and compiling chrono-stratigraphic frameworks, and present two case studies. For more detailed and comprehensive overviews on the principles of stratigraphy and mapping, we refer the volcanological community to recent compilations [1-6].

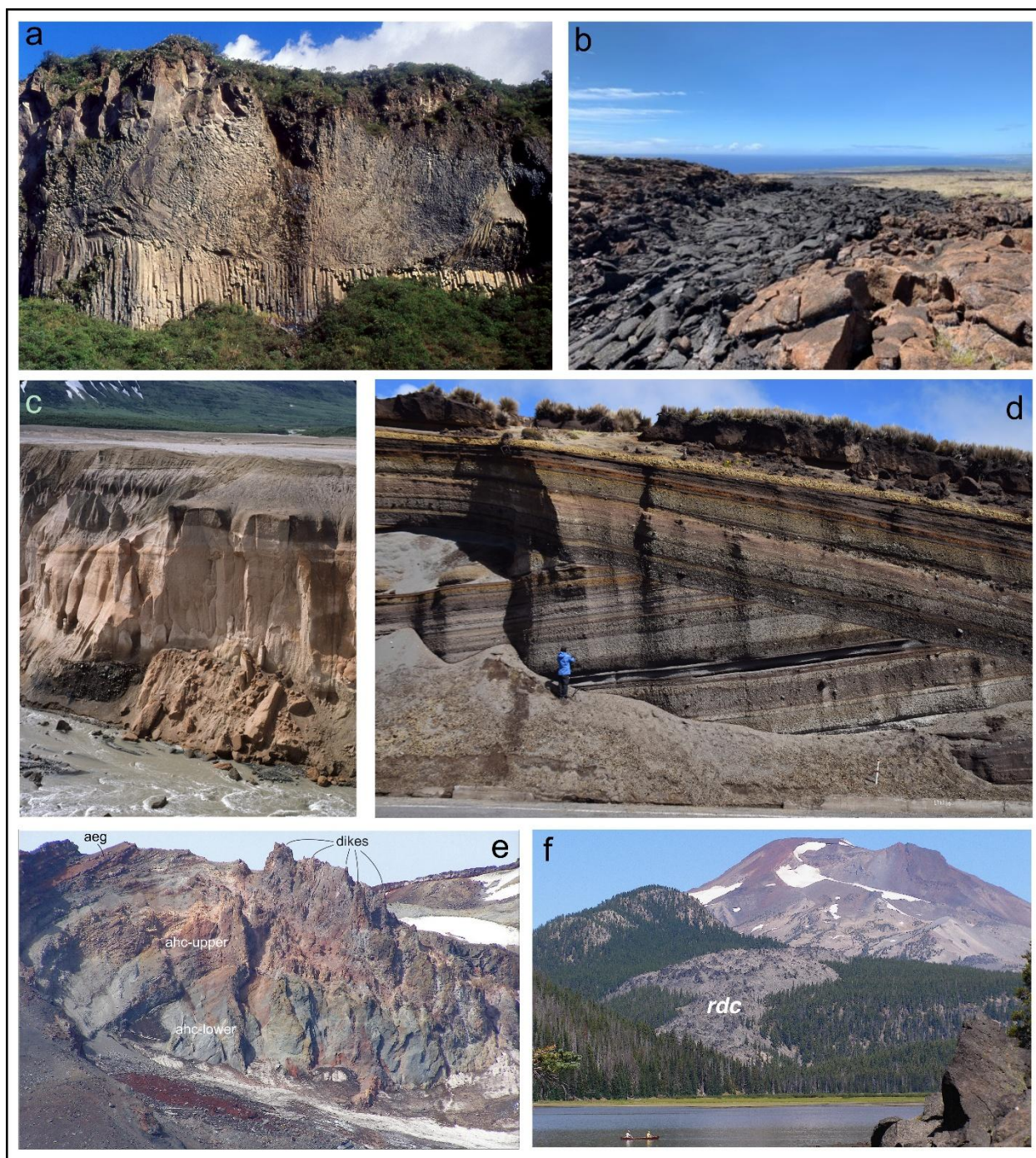


Figure 1: Outcrop-scale photos of a range of volcanic rocks and deposits **(a)** Las Juntas andesite lava flow, Tungurahua, Ecuador, showing cooling fractures at variable scales, including columnar jointing at the base; **(b)** Photo of lava flows in the Southwest Rift Zone of Kilauea, Hawai'i, USA, demonstrating the principle of superposition, and differences in weathering and vegetation based on their relative ages. The dark black lava flow erupted in 1823 CE; it overlies the reddish-brown lava flow (bottom right), and both flows overlie an older lava flow (back right) that is well vegetated with grass; **(c)** Valley-filling and sintered ignimbrite deposits, Valley of 10,000 Smokes, Alaska, USA; **(d)** Angular unconformity in a sequence of

pyroclastic fallout deposits at Totorillas, Chimborazo, Ecuador; **(e)** Coherent andesitic lava flows (aeg) overlaying andesitic pyroclastic facies (ahc), adjacent to intrusive complex of Hodge Crest at Prouty headwall, South Sister, Oregon, USA; **(f)** Rhyolite lava flow of Devils Chain (rdc), South Sister, Oregon, USA. For unit abbreviations of photos **(e-f)** and sequence interpretations, see Case Study 1. All photos by the authors.

Planning and preparing for fieldwork

The level of detail and amount of time required when mapping and establishing stratigraphy will depend on the objectives and desired end-products of the study. For example, a geologic map of an entire volcanic complex documenting its complete 100s-kyr-time-volume-compositional record can take a decade (**Case Study 1**); and a Holocene stratigraphic profile that compiles frequency-magnitude relationships of past eruptions to support a hazard assessment can take several years to complete (**Case Study 2**). However, an isopach map of a single widespread pyroclastic deposit, or a detailed profile of strata within deposits that document changing behavior during a single eruption may take less time. Regardless of the scale and scope of fieldwork that underlies the mapping, appropriate field kit and preparation are important in being able to achieve the mapping and scientific objectives safely and thoroughly, while considering ethics of fieldwork, especially for work in sensitive areas, and engaging in appropriate collaborations (**Fig 2 / How-To Box 1**).

[Additional Reading QR3: "Collaborations"]

Field kit and preparation	Health and Safety (depending on fieldwork location)
Essential kit	<ul style="list-style-type: none"> - Canteen/water bottles - Appropriate footwear, clothes and accessories for a variety of meteorological conditions (sunscreen, sunglasses, hat, rain gear, etc.) - Insect repellent, bear spray, antihistamines - Overnight gear (if necessary): tent, sleeping bag, etc. - Flashlight/headlamp - Hard hat, sturdy gloves, goggles/safety glasses - First-aid kit, emergency numbers and contact details, water purification system, medication - For remote field work: communication device appropriate for location (e.g., satellite phone, InReach, emergency beacon, radio) - Communication and emergency locator beacon - Oxygen, acid gas, N95 masks (depending on environment) - Walking sticks - EpiPen, any other life-saving medication - ...
Advanced kit (depending on objectives)	Essential preparation
<ul style="list-style-type: none"> - Tablet/smartphone with installed mapping or stratigraphy apps (e.g., GeoMapApp, StraboSpot, QField for QGIS) - Water spray flask to reveal sedimentary structures - Lacquer peels for high-resolution outcrop observation and sampling - Tarpaulin sheet, field balance, sieves, calipers, etc. - Drone - Laser Rangefinder - Binoculars - Portable XRF - ... 	<ul style="list-style-type: none"> - Literature review - Base maps from remote sensing or previous mapping studies - Identify target locations/areas, e.g. using topographic maps, Google Earth or existing literature - Liaise with (local) colleagues and communicate objectives and planning - Obtain appropriate permits (visa, research permit, national park entry, etc.). Note that some of these may require planning well in advance. - Prepare risk assessment to include both natural (fauna, flora, geohazards) and human-induced risks - ...

Figure 2 (How-To Box 1): Summary overview of things to consider before going the field, including kit to take and precautionary preparations

From fieldwork to compiling a map

A first-order task when mapping is identifying major constructive and destructive geomorphic features (e.g. (strato)cones, lava flows, tuff rings, maars, landslide scars) and establishing their distributions. Geomorphic features, drainage patterns, regional faults, and structural lineaments are all considered in understanding the topography of the landscape. Remote sensing data (satellite imagery, lidar datasets, and aerial photography) and digital elevation models derived from the imagery are useful, and topographic and road maps essential. Careful consideration of all the imagery and maps permits some degree of evaluating accessibility of areas and outcrops prior to fieldwork and is invaluable once “on the ground.”

Most geologic mapping of volcanoes and stratigraphic correlations are initially based on a lithostratigraphic approach, meaning that rocks are distinguished, characterized and preliminarily assigned to units based on lithological properties, stratigraphic positions and distributions. It is important to clearly describe every relevant feature at the scale of the outcrop and deposit, and of individual samples or clasts, and to separate these descriptions as much as possible from genetic interpretations. Such complete descriptions provide a solid basis for a unit’s final definition, its spatio-temporal position, and interpretive conclusions. Units can be assigned as finely as they can be distinguished. Some lavas can be mapped as individual flows, others as packages of flows derived from the same vent and eruptive episode. Fragmental and sedimentary deposits of similar lithological properties are referred to as facies, but a single facies may repeat across time and stratigraphy and occur independently in unrelated spatial contexts across a map. A formal lithostratigraphic unit is discrete and has clearly defined upper and lower boundaries within a stratigraphic succession but may contain internal facies variations. Such variations can be especially important in volcanic sequences, where characteristics of units can change with distance from vent [1-4].

Lithostratigraphic units can be placed in a chronological context first by establishing field-based stratigraphic relations, then by augmenting those with geochronology (see below). The former involves correlation of outcrop remnants and evaluation of how different units are juxtaposed. Position and distribution of the units relative to the landscape is also an important consideration. For instance, it is common for older lava flows to remain as ridge-capping remnants high above younger lavas that fill an adjacent glacial or river-carved valley below [6]. Upper and lower limits of identified units may take the form of paleosols, erosive surfaces, or unconformities, which represent breaks in time or quiescence between eruptions. In some cases, unit boundaries are subtle and only revealed through detailed analyses of chemical or mineralogical composition or geochronology [2]. In the last few decades, mapping of pyroclastic volcanic sequences has sometimes included the concept of unconformity bounded stratigraphic units (UBSUs), which allows identification of an unconformity hierarchy, and hence, of the enclosed volcanic successions [3]. For example, a short pause or simple change in style during an eruption will produce depositional breaks that can be traced only within the deposits of that specific eruption. On the other hand, catastrophic destructive phenomena such as landslides and caldera collapse can quickly cause large-scale unconformities. Such unconformities therefore do not really represent a significant hiatus in time and there is no consensus whether they should be considered to bound stratigraphic units [1-2]. Given the strong lateral and vertical facies variations that are characteristic of many fragmental

volcanic deposits, including those representing a single eruption, it remains important to start from a lithologic and facies-based approach in compiling maps and stratigraphic profiles, especially in volcanic terrains that have not yet been mapped in detail. Identifying and mapping successive products of each vent on a volcano or in a volcanic field provides a first-order clustering of map units useful in documenting eruptive history. Lavas, PDCs, pyroclastic falls, epiclastic deposits etc., might all be products of the same eruptive episode. Formal assignment of stratigraphic hierarchy into groups, formations and members can only happen when one is adequately confident that all units have been distinguished and defined, and this happens only late in the iterative process of compiling a geologic map and/or chronostratigraphic framework supported by adequate compositional and geochronological data.

Key descriptive features

Some key features to consider when describing volcanic rocks and deposits at outcrops include how surrounding topography has influenced distribution of lavas and fragmental deposits. Other considerations include rock texture, morphology, crystallinity or phenocryst content (if coherent), deposit granulometry, sorting and componentry (if volcanoclastic), vesicularity, mineralogy, depositional structures, thicknesses, and any other defining characteristics. Some of these, and a selection of appropriate sampling strategies, are listed in **Figure 3 / How-To Box 2**. Following a systematic procedure with a clear separation of description and interpretation will help to assign correct genetic names to any volcanic package, including most of those where the original lithofacies might be heavily modified, deformed, or completely overprinted by alteration [5].

Describing and sampling volcanic deposits in the field	
<p>Descriptions</p> <p>Large scale</p> <ul style="list-style-type: none"> - Geomorphology of the surrounding terrain - Size, orientation and nature of the outcrop - Structural features - ... <p>Deposit / outcrop-scale</p> <ul style="list-style-type: none"> - Nature of contacts, soil development, ... - Deposit/unit thickness and possible lateral variations - Lava flow morphology and textures, presence of cooling fractures, ... - Sedimentary structures (layering, cross-bedding, ...) - Degree of lithification (welding, cementation, ...) - Grain size : mode, minimum, maximum grain size - Sorting and grading, any vertical or horizontal variations - Clast componentry (juveniles, crystals, accessory clasts, ...) - ... <p>Sample / clast-scale</p> <ul style="list-style-type: none"> - Colour - Morphology - Texture - Vesicularity - Mineralogy - ... 	<p>Sampling strategies</p> <p>For mineralogy and (bulk) geochemistry</p> <ul style="list-style-type: none"> - Coherent facies: fist-size sample, from the core or top of the unit/flow, without visible weathering or secondary minerals. Some features like vesicularity and mineralogy may vary widely across the flow, and from proximal to distal locations. - Pyroclastic facies: vertical channel samples across the entire thickness of a deposit or subsection. Individual clasts can be collected with a stratigraphic context. Avoid clast breakage by loosely scraping the outcrop surface if possible. Sample top units first to avoid cross-contamination. <p>For geochronology</p> <ul style="list-style-type: none"> - ¹⁴C dating: individual pieces of charcoal or other organic material. Bulk soils to be avoided if possible. Large trunks of trees sampled on the outside represent their youngest age when incorporated in a deposit. - Ar-Ar dating: groundmass or crystals. The amount necessary will depend on rock type, texture, and crystallinity, and can range from a few tens of grams to a kilogram of material. Avoid glassy, vesicular rocks. - Cosmogenic dating: groundmass or crystals (depending on the isotope system used), and usually requires several hundred grams in an open setting (not being shielded by high topography). - Paleomagnetic drilling of rocks can be used for correlations and in the right context provide age constraints. Contingent upon skill with a drill and ability to orient and extract cores to be measured in a magnetometer. <p>For componentry / grain size analysis</p> <ul style="list-style-type: none"> - Grain size and componentry analyses on coarse fractions (>4 mm) of pyroclastics can be performed in the field. Take finer fractions to the laboratory for further analysis.

Figure 3 (How-To Box 2): Non-exhaustive overview of features to describe when mapping volcanic rocks and deposits at a range of scales in the field, and some practical aspects to consider when sampling for

different purposes. Several features described in the field, such as sorting, modal abundance of components, or roundness of clasts, are ideally estimated using visual comparison charts.

A brief overview of key volcanic rocks and deposits, with reference to relevant chapters in this volume, is provided in **Table 1**. For detailed overviews of eruption processes, emplacement mechanisms, and resulting deposit features, we refer to these relevant chapters, and [1].

Table 1. Overview of key categories of volcanic rocks and deposits. For an exhaustive overview of classes of coherent and volcanoclastic rocks and their essential characteristics, we refer to relevant chapters in this volume and [1].

Deposit observed (described)	Depositional mechanism (interpreted)	Chapter
Coherent lava	Lava flow/dome	Part 3, Chapter 3.1-3.2
Well-sorted pyroclastic deposit	Pyroclastic air fall (aggradation)	Part 3, Chapter 4.3
Plastic flattened clast, or impact-/sag-structure under clast	Ballistic transport of bomb or block	Part 3, Chapter 4.3
Poorly sorted pyroclastic deposit	Dilute pyroclastic density currents (stepwise aggradation / fluid-escape / traction-dominated flow boundary zone)	Part 3, Chapter 4.4
	High-concentration pyroclastic density currents (stepwise aggradation/ granular-flow/ fluid-escape dominated flow boundary zone)	Part 3, Chapter 4.3
Poorly sorted volcanoclastic sediment	Low-concentration lahars	Part 3, Chapter 5.1
	High-concentration lahars	Part 3, Chapter 5.1
	Debris-Avalanche	Part 3, Chapter 5.4
	Moraine	Part 3, Chapter 2.3
Well-sorted volcanoclastic sediment	Aeolian remobilized ash	Part 3, Chapter 5.2
Poorly or well-sorted breccia with altered matrix	Hyaloclastite	Part 3, Chapter 2.2-2.3

Map units characterized in the field using a hand lens are further evaluated petrographically and compositionally in the laboratory, and this laboratory work may be synchronous with field mapping over several seasons in an iterative process (**Case Study 1**). From macroscopic to microscopic scales, observations of vesicularity (vesicle abundance and shape, vesicle size distribution), crystallinity (crystal abundance, shape and organization, crystal size distribution, mineral paragenesis), and groundmass (presence of microlites, glass, devitrification), along with degree and type of alteration can provide relevant information about volcanic rocks of interest. Defining eruptive units and timeframes, however, requires ample additional compositional and geochronological data. The Sm-Nd, K-Ar, ^{40}Ar - ^{39}Ar , and U-Th-Pb isotopic systems are generally applied to date Pleistocene-age and older volcanic rocks, whereas U-series, ^{14}C , ^{40}Ar - ^{39}Ar , and cosmogenic dating methods, such as ^3He and ^{36}Cl , are suitable for Pleistocene and Holocene age volcanic rocks [7].

[Additional Reading QR4: "Chronology methods"]

Temporal (e.g., chrono-stratigraphic) history is often put into context with magma compositions, source vents/volcanoes, deposit distributions and volumes, and eruptive styles and magnitudes. Temporal information that is crucial to understanding eruptive histories and long-term volcano evolution includes eruption recurrence intervals, and whether eruptions tend to occur as clustered events, statistically individual events, or a mix over a volcano's lifetime. Conventionally, ages are integrated with location of source vent to determine lava and pyroclastic density current extents and airfall tephra dispersal patterns. This helps in constraining areas that have been inundated by products from effusive and explosive eruptions across local to regional scales through time, and yield insights into edifice growth versus collapse and erosion. Integrating the spatio-temporal framework with composition and mineral data, such as mafic versus silicic magma contributions, is also useful for clarifying volcano source provenance, and interpreting magma plumbing systems that can experience changes in magma genesis, flux, storage zone development, and transport [8]. Understanding the plumbing system provides a proxy by which to better interpret seismic and other geophysical data at active volcanoes [9] or at volcanoes prospected for geothermal exploitation.

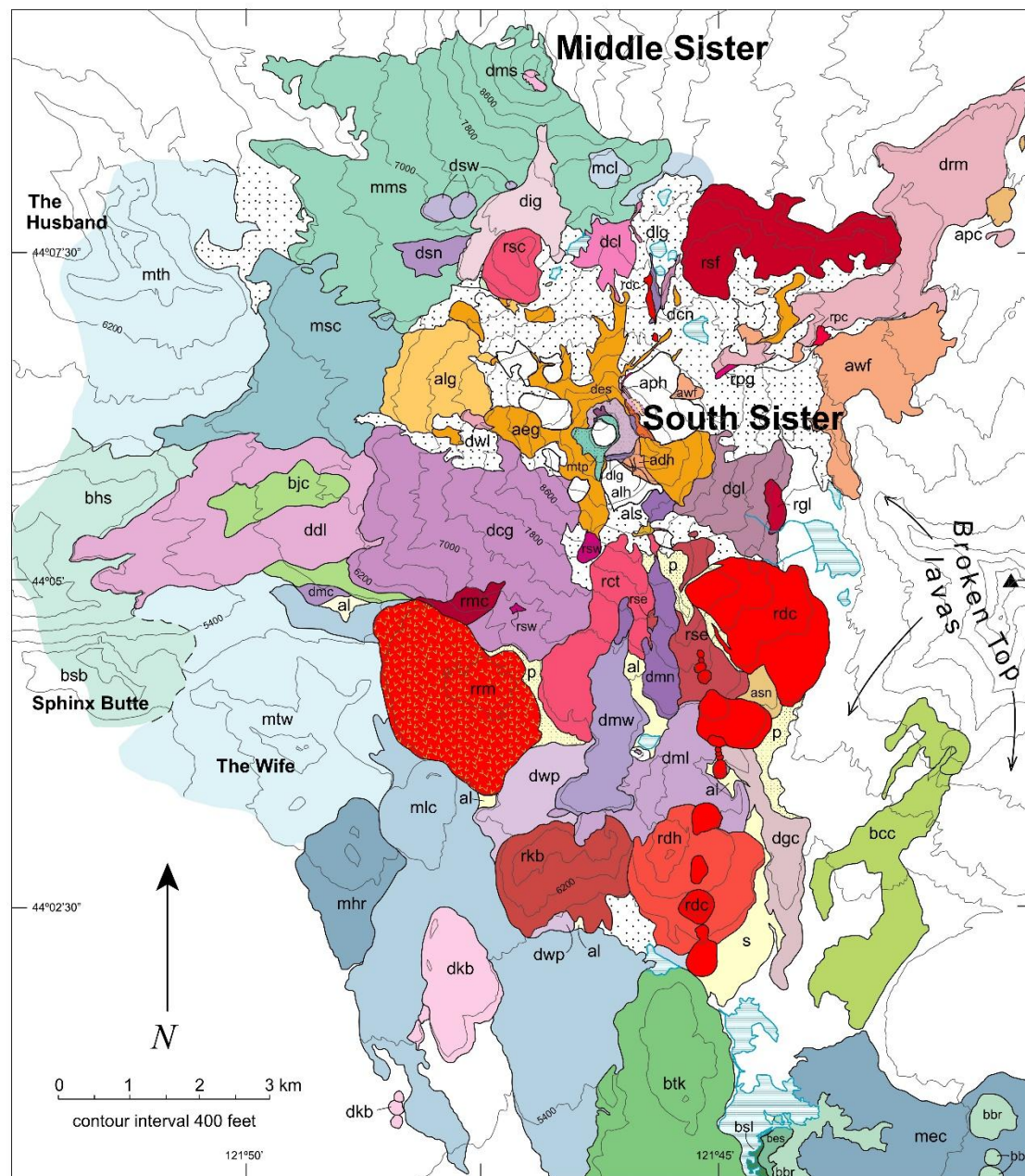
[Additional Reading QR5: "Magma plumbing systems, petrological monitoring"]

Case Study 1: Geologic map of South Sister, Oregon, USA

The Three Sisters complex is a cluster of glaciated stratovolcanoes (North, Middle, and South Sister) in the Cascade Range of Oregon, USA. Glacial erosion has significantly shaped the morphology of this complex; however, the volcanoes have been sufficiently active in the Quaternary for most landforms to be the result of constructional processes. Uplift centered about 5 km west of South Sister was detected by satellite and GPS between the mid-1990s and mid-2000s and was interpreted to be caused by a magmatic intrusion. Hildreth et al. [10] present a detailed geologic map at 1:24,000 scale, covering an area of exclusively Quaternary volcanic rocks and derived epiclastic deposits. The map was constructed during about 200 days of fieldwork, mostly on foot, spanning a period of almost 10 years. In total, 145 volcanic units were mapped, with each analyzed for petrography and geochemistry in an iterative process that gradually resulted in the published map. Part of those petrological and geochemical investigations were completed as part of topical studies. The chronostratigraphic framework is constrained by ^{40}Ar - ^{39}Ar dating on most pre-Holocene rocks in combination with field-established stratigraphic relations to piece together the complete volcano history [10].

[Additional Reading QR6: “Three Sisters, Oregon, USA”]

North Sister is a glacially dissected basaltic andesite edifice that is part of the mafic periphery of the complex and had its main constructive period between ~120 – 45 ka. During this period, several major unconformities are identified, indicating multistage edifice growth. Middle Sister, an andesite-basalt-dacite cone, was built during the interval from 48 to 14 ka but mostly between 25 and 18 ka, overlapping in time with South Sister. Activity at South Sister began with eruption of predominantly rhyolitic lava flows and domes between ~50 – 30 ka. Toward the end of this period, rhyodacitic lavas also appear, followed by construction of the main andesitic edifice [11]. This relative sequence is visible in **Figure 4**, with older rhyolite units at the southern and northern base of the edifice (reds), followed by dacites (purples) and andesites erupted from the summit (oranges). The youngest activity, however, is rhyolitic, with the emplacement at ~2.2 ka of lava flows and tephra deposits (unit rrm) and at ~2 ka of dike-fed lavas along a N-S trending chain of eruptive vents (unit rdc; **Figure 4**; [10, 11]).



Tephrostratigraphy and tephrochronology

Tephrostratigraphy is the stratigraphic reconstruction of a sequence of pyroclastic deposits (fallout and PDC) that are usually more spatially widespread than products of effusive eruptions. Documenting tephra distribution provides opportunities to estimate deposit volumes and eruption style, and thus corresponding magnitudes of these eruptions [E18]. Whereas a volcano geologic map represents the long-term evolution of a volcanic system or complex, hazard-informing tephrostratigraphic frameworks are most often limited to the latest Quaternary, due to limited preservation potential of non-consolidated pyroclastic deposits in humid climates or previously glaciated regions. When absolute geochronological information can be integrated with a tephrostratigraphic framework (i.e. tephrochronology), tephrostratigraphy becomes an effective tool to constrain eruption recurrence intervals, as well as long-term eruptive rates (10^2 – 10^6 years) at the scale of an individual volcano or complex, or of a volcanic region. Because tephra deposits, particularly from widespread tephra fallout, are emplaced near-instantaneously (generally, hours to months) in different sedimentary environments (terrestrial, lacustrine, marine, glacial), they have the potential to form an isochron or ‘time-horizon’ marker bed in the stratigraphic record. A well-defined absolute age of a well-characterized (“fingerprinted”) tephra deposit may then be transferred across sedimentary profiles, which may be studied in different disciplines beyond volcanology, including paleoecology, palaeoclimatology, archaeology, etc. [12]. For mapping purposes, tephrostratigraphic records are most useful when the deposits can be correlated to the vent(s) from which they initiated.

To support correlations between sedimentary profiles and environments, and potentially transfer ages across them, thorough documentation of physical and chemical characteristics of a tephra deposit is required [13]. Modern mobile applications can be useful in systematically recording all the useful information and measurements and directly import them into a centralized and geo-referenced database. Ideally, properties that are used to uniquely fingerprint and correlate tephra deposits are independent of distance from eruptive source or deposit preservation conditions. Lithological descriptions in the field or laboratory (e.g., on sediment cores) include basic characterizations such as thickness, color, grain size distribution, depositional fabric, and componentry (e.g., proportion of juvenile and accidental lithic clasts, mineral assemblage). Some of these features can, however, change with distance from source, and for this reason, geochemical fingerprinting is often essential to fully characterize tephra deposits and support correlations.

Geochemical fingerprinting is usually performed on juvenile components (e.g. volcanic glass shards and phenocrysts). Unlike the bulk composition of a pyroclastic deposit, glass and/or mineral compositions in deposits from a particular eruption are more likely to be distinct from those of other eruptions (from the same or other volcanoes) due to processes of magmatic evolution. Both silicate and Fe-Ti oxide minerals have been successfully used to fingerprint and correlate tephra deposits (**Case Study 2**). However, because distal to ultra-distal tephra deposits (100s–1000s km from source) are generally dominated by volcanic glass shards, and because the glass fraction tends to also dominate proximal sequences, geochemical fingerprinting of glassy groundmass remains the most common tool to support tephrochronological correlations [12, 14]. Improvements in micro-sampling and analytical techniques on a limited number of individual, small glass shards have allowed significant progress in studies of ultra-

distal tephra deposits that may be detected as cryptotephra in glacial, lacustrine, or other sedimentary systems [14, 15].

Accurately identifying sources and correlating (crypto)tephra layers relies on the availability of a database of chemical compositions of widespread, regional correlative deposits. Such databases may be used to identify chemically similar, correlative tephra using statistical tools such as Principal Component Analysis or k-means clustering. Even with geochemical fingerprinting techniques, however, distinguishing between different eruptions may still be difficult, as chemical compositions of products from a single volcano tend to be overlapping. Thus, additional constraints from field observations, physical characterizations of tephra, and other data such as componentry, may help support correlations.

[Additional Reading QR7: “Tephrostratigraphy and Tephrochronology: methods, databases and case studies”]

Construction of a solid chrono-stratigraphic framework, and volcano-geologic map, is founded on rigorous field observations and the ability to investigate adequate outcrops and samples. In some cases, finding suitable material for dating poses a challenge. For example, radiometric dating systems generally use specific minerals, appropriate groundmass, or charcoal that are not always present in volcanic deposits of interest. As a result, it may be challenging to obtain absolute chronologies for major evolutionary stages of a volcanic system or for each individual lithostratigraphic unit or eruption. Even when suitable material is available for radiometric dating, if a sequence contains an overabundance of deposits emplaced at rates faster than the accuracy of the dating technique, it is not feasible to date every single unit. As a result, eruption history databases [16] do not always contain all the relevant information that could be retrieved from a (Holocene) stratigraphic framework, and care should be taken when using them as a basis for probabilistic hazard assessment [E3].

Case study 2: The post-glacial tephrostratigraphic framework of Mocho-Choshuenco volcano, Chile.

Mocho-Choshuenco, a volcanic complex in the Southern Volcanic Zone of the Andes in southern Chile, was severely glaciated during the Last Glacial Maximum at ~25-16 ka. On-land tephrostratigraphic records comprise unconsolidated volcanic deposits and soils that are easily eroded, and are thus typically limited to the post-glacial period. Only marine or rare lacustrine exposures reveal longer-term records of repeated volcanic ash deposition during glacial periods. Rawson et al. [17] present a high-resolution tephrostratigraphic reconstruction of Mocho-Choshuenco’s post-glacial history based on detailed field observations from ~400 locations, including distal tephra sections up to 70 km from the central edifice. Outcrop exposure and deposit preservation are limited due to dense vegetation and high annual rainfall, so smaller-scale deposits are likely missing from the record. Field observations were combined with geochemical (glass and Fe-Ti oxide major and minor element composition) and geochronological (radiocarbon) data and checked against each other in an iterative process to compile the composite stratigraphy. A Bayesian statistical approach on this composite profile, into which several units have multiple radiocarbon dates associated with them, allowed compiling an age model and assigning age probability functions to each individual unit in the profile. The most widespread deposits were identified

in at least 10 different locations, and isopach (equal thickness) and isopleth (equal maximum grain size) maps allowed estimates of eruption magnitudes [E18].

The post-glacial tephrostratigraphic record at Mocho-Choshuenco includes 25 well-defined and chemically fingerprinted lithostratigraphic units (**Figure 5**) some with sub-units defined by facies variations, and numerous poorly preserved interbedded scoria fallout deposits. A total of ~75 discrete post-glacial eruptions are identified, spanning a history of ~16.5 kyr of explosive activity, and corresponding to an average eruption frequency of ~220 years. About half of the eruptions originated from (monogenetic) scoria cones along the flanks of the complex, and four were Plinian eruptions of magnitudes between 5.0 and 5.7 (**Figure 5**), that produced widespread tephra fallout and/or PDC deposits of andesitic to rhyodacitic compositions. Since the last major eruption (~ 1.7-1.5 ka) the ten youngest units are predominantly scoria fallout deposits of andesitic compositions, including the most recent historical eruption in 1864 CE [17].

[Additional Reading QR8: “Southern and Austral Volcanic Zone, Chile”]

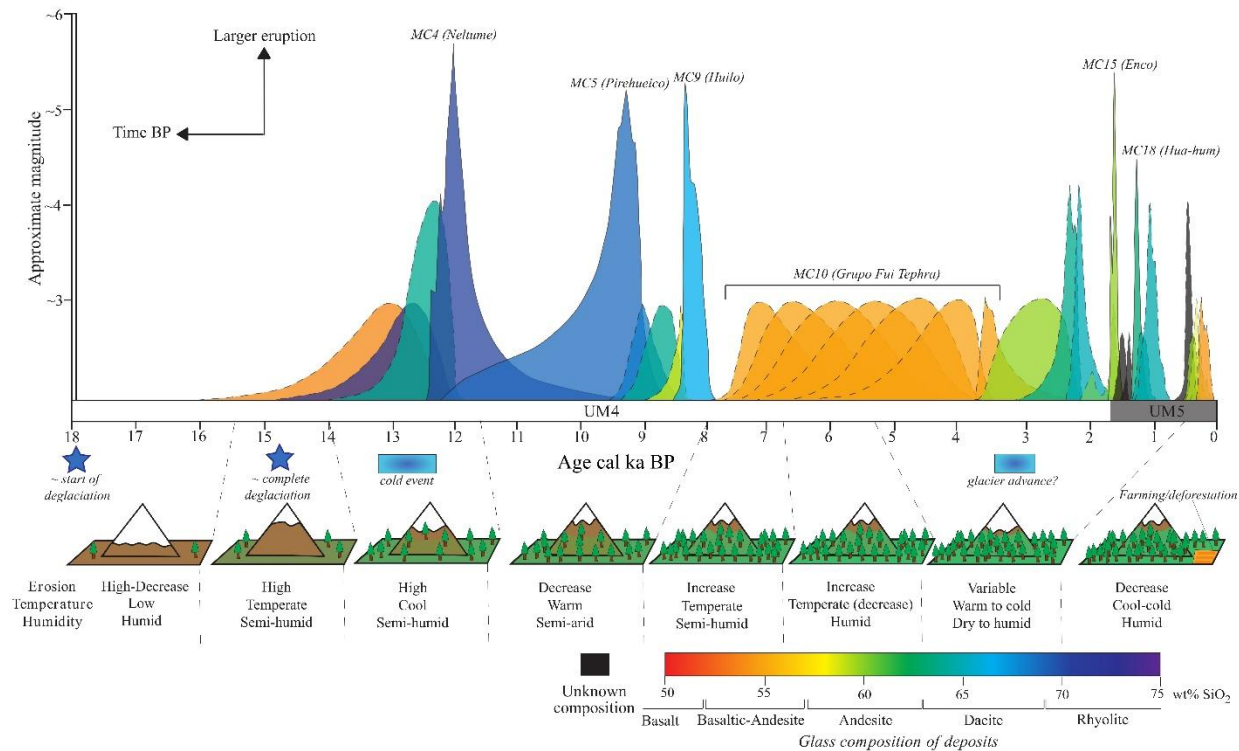


Figure 5 Summary of explosive eruptions from Mocho-Choshuenco since the onset of deglaciation at ~18 ka. Each of the 25 chemically and stratigraphically constrained units are represented by their modeled age probability function, with the peak height scaled to the estimated eruption magnitude and color-coded by chemical composition. Note that major Plinian eruptions are not evenly spaced in time, which is attributed to a response of the magmatic plumbing systems to deglaciation. Erosion rates, temperature, humidity and vegetation density inferred from paleoenvironmental reconstructions from a lake sediment core ~90 km South of Mocho-Choshuenco (for references, see Additional Reading). Figure modified from [17].

Preservation bias: insights from modern eruptions

Recent eruptions and careful tracing of their deposits in near-real-time help in evaluating preservation potential and bias in the geological record. Three examples follow: (1) The small-to-moderate 2011-12 subplinian eruption of Cordón Caulle, Chile, dispersed volcanic ash over Patagonia in a lobate dispersal pattern and with multiple vertical grain-size variations in the deposits due to the long-lasting and pulsating nature of the eruption. The present-day deposit is poorly or not preserved except in localized, near-vent areas due to post-depositional erosion and remobilization, including by wind. This suggests that eruptions of pyroclastic material smaller than VEI or Magnitude 3 are unlikely to be preserved in the geological record, except in lake sediment and peat cores. Even in lake sediment cores, interpretations of volcanic ash-layer grain size and thickness should be treated with caution. Tephra from the 2011-12 Cordón Caulle eruption was dispersed entirely eastward of the volcano, yet a volcanic ash layer was found in sediments of Lake Puyehue located to its west due to in-washing from the lake's catchment [18]. Therefore, this ash was not formed as a primary pyroclastic deposit but was epiclastic in origin. Complicating distribution analysis still further, the grain size and thickness of this ash increased with distance from source, likely because of intra-lake currents distributing the sediment into different sub-basins of the lake [18].

[Additional Reading QR9: "Modern eruptions"]

(2) In Iceland, three distinct lava flows erupted from a fissure at Fagradallsfjall during three different eruptions between 2021 and 2023. The flows overlap with each other and are likely to leave a mostly coherent lava flow in the geological record of interbedded massive and auto-brecciated facies. From an operational monitoring perspective, they are considered different eruptions because the pause in activity between them was more than three months [16]. However, on a geologic map or in a stratigraphic profile, the products of these lava flows would likely be grouped into one lithostratigraphic unit and interpreted as the products of one eruption.

(3) The 2022 paroxysmal submarine eruption of Hunga Tonga-Hunga Ha'apai demonstrated the generally poor knowledge of submerged or partially submerged volcanoes and their underestimated hazards. Mapping such volcanoes represents a major challenge, as underwater geological surveying is almost entirely based on high-resolution bathymetric reconstructions, limited visual inspections, and sampling by remotely operated vehicles [19].

Recent advances

Since the end of the late 2000s, Uncrewed Aerial Vehicles (UAVs), commonly referred to as drones, have revolutionized fieldwork, especially for volcanic mapping [20]. UAVs enhance safety and improve accessibility to rugged, often unstable and steep volcanic terrains. The evolution of propulsion systems, battery technology, as well as the miniaturization of sensors and the improvement of data transmission capabilities have collectively propelled drones to operate at distances several kilometers from active vents and hazardous areas.

The use of a variety of sensors, including visible RGB, thermal, multispectral, and lidar, enables UAVs to capture high-resolution imagery, down to centimeter scale, along with precise positioning using Real Time

Kinematics (RTK). This facilitates the creation of georeferenced rasters such as orthomosaics and digital elevation models using Structure from Motion (SfM) photogrammetry techniques (**Figure 6**). Moreover, drones can reconstruct structures and landscape in 3D with unprecedented accuracy, which is helpful in better understanding volcanic successions and underlying processes.

One of the major advances associated with UAVs is the ability to collect data during volcanic events that can be processed in near-real-time, enabling volcanologists to quickly assess volcanic hazards and update existing maps. Drones are now extensively used to produce maps of lava fields and estimate dome growth. This is also possible because UAVs are often more cost-effective than traditional aerial surveys, which is extremely helpful for volcanic observatories working on a limited budget.

[Additional Reading QR10: "Recent advances"]

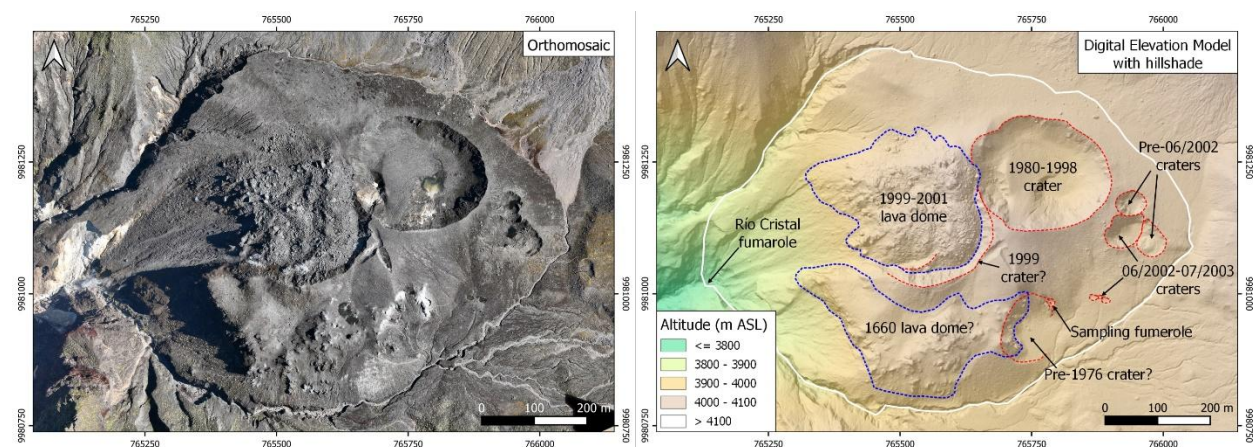


Figure 6 Orthomosaic (left, GSD 11.4 cm/px) and Digital Elevation Model with hillshade (right, GSD 23.4 cm/px) of Cristal dome complex at Guagua Pichincha volcano, Ecuador. The red dashed lines correspond to the crater rims and the blue dashed lines to the lava domes. The coordinate system is WGS 84, UTM zone 17S.

Summary

Geologic maps and stratigraphic reconstructions of volcanoes provide fundamental information for studies on volcanic hazards and probabilistic hazard assessments that may be used by volcano observatories and other agencies to inform the public and other stakeholders. Such work also supports other volcanological studies that require an understanding of the evolution of volcano-magmatic systems; it can support surface exploration studies for geothermal development; and it can be used in ancient volcanic terrains for identifying mineral resources. Mapping and stratigraphy rely on rigorous fieldwork that ultimately constructs time-volume-composition records that characterize magnitudes, styles, and periodicity of all past activity. Recognizing the full range of past behavior of an edifice or volcanic field provides an essential complement to real-time instrumental monitoring.

When mapping a particular volcanic area, every piece of evidence, from macroscopic to microscopic scale, becomes relevant to achieve a rigorous and precise interpretation. Modern technologies simplify field preparations, including the selection of targeted areas and interpretations of large-scale structures and geomorphological features. Field observations are important in distinguishing contact relations and unconformities of variable scales, which are critical to understanding the stratigraphic sequence, and which must be confirmed with geochronological data. Detailed geomorphological and structural studies must be done to detect possible regional controls on volcanic morphology and activity. An exhaustive lithofacies analysis should be complemented with geochemical data to support stratigraphic correlations. Meaningful definition of eruptive units and temporally clustered eruptive groups requires ample compositional and geochronological data. Laboratory work is synchronous with field mapping and typically iterative over several seasons.

Construction of tephrostratigraphic frameworks is reliant on geochemical fingerprinting to verify correlations. This fingerprinting may include a combination of glass or mineral major- and trace-element chemistry, and componentry analysis. Advances in sample preparation methods and analytical techniques now allow correlating volcanic ash layers as much as 1000s of kilometers from source. Statistical analyses and machine learning techniques can help refine correlations of large datasets, but should still be verified by field constraints, especially in cases where there are similar chemical compositions in a stratigraphic sequence. Importantly, study of tephras aims not only at mapping timelines but at linking them to vent sites on the edifice, correlating the chronology of cone lavas to that of fragmental deposits. Mapping and stratigraphic studies together can develop an integrated stratigraphic, chronological, structural, geomorphic, and petrologic framework that, combined, document comprehensive eruptive histories.

Disclaimer

Any use of trade, firm, or product names is for descriptive purposes only and does not imply endorsement by the U.S. Government.

References [1-20]

- [1] R. Cas, G. Giordano, and J. V. Wright, *Volcanology: Processes, Deposits, Geology and Resources*, Springer Textbooks in Earth Sciences, Geography and Environment. Springer International Publishing, 2024. doi: [10.1007/978-3-319-66613-6](https://doi.org/10.1007/978-3-319-66613-6).
- [2] J. Martí, G. Groppelli, and A. Brum Da Silveira, Volcanic stratigraphy: A review, *Journal of Volcanology and Geothermal Research* 357 (2018) 68–91, doi: [10.1016/j.jvolgeores.2018.04.006](https://doi.org/10.1016/j.jvolgeores.2018.04.006).
- [3] F. Lucchi, On the use of unconformities in volcanic stratigraphy and mapping: Insights from the Aeolian Islands (southern Italy), *Journal of Volcanology and Geothermal Research* 385 (2019) 3–26, doi: [10.1016/j.jvolgeores.2019.01.014](https://doi.org/10.1016/j.jvolgeores.2019.01.014).
- [4] K. Németh and J. Palmer, Geological mapping of volcanic terrains: Discussion on concepts, facies models, scales, and resolutions from New Zealand perspective, *Journal of Volcanology and Geothermal Research*, 385(2019) 27–45, doi: [10.1016/j.jvolgeores.2018.11.028](https://doi.org/10.1016/j.jvolgeores.2018.11.028).
- [5] R. Cas, J. V. Wright, and G. Giordano, Terminology for Volcanic Deposits and Rocks, in: R. Cas, G. Giordano, and J. V. Wright (Eds.), *Volcanology: Processes, Deposits, Geology and Resources*, Springer Textbooks in Earth Sciences, Geography and Environment, Springer International Publishing, 2024, pp. 1121–1160. doi: [10.1007/978-3-319-66613-6_14](https://doi.org/10.1007/978-3-319-66613-6_14).
- [6] B. van Wyk de Vries, D. Karatson, C. Gouard, K. Németh, V. Rapprich, and E. Aydar, Inverted volcanic relief: Its importance in illustrating geological change and its geoheritage potential, *International Journal of Geoheritage and Parks* 10 (2022) 47–83, doi: [10.1016/j.ijgeop.2022.02.002](https://doi.org/10.1016/j.ijgeop.2022.02.002).
- [7] J.G. Shellnutt, S.W. Denyszyn, and K. Suga (Eds.), *Methods and Applications of Geochronology*, Elsevier, Amsterdam, 2024
- [8] J. Blundy and K. Cashman, Petrologic Reconstruction of Magmatic System Variables and Processes, *Reviews in Mineralogy and Geochemistry* 69 (2008) 179–239, doi: [10.2138/rmg.2008.69.6](https://doi.org/10.2138/rmg.2008.69.6).
- [9] G. Re, R. A. Corsaro, C. D’Oriano, and M. Pompilio, Petrological monitoring of active volcanoes: A review of existing procedures to achieve best practices and operative protocols during eruptions, *Journal of Volcanology and Geothermal Research* 419 (2021), 107365, doi: [10.1016/j.jvolgeores.2021.107365](https://doi.org/10.1016/j.jvolgeores.2021.107365).
- [10] W. Hildreth, J. Fierstein, and A.T. Calvert, Geologic map of Three Sisters volcanic cluster, Cascade Range, Oregon: U.S. Geological Survey Scientific Investigations Map 3186, 2012, pamphlet 107 p., 2 sheets, scale 1:24,000, Available at <https://pubs.usgs.gov/sim/3186/>.
- [11] J. Fierstein, W. Hildreth, and A. T. Calvert, Eruptive history of South Sister, Oregon Cascades, *Journal of Volcanology and Geothermal Research* 207 (2011) 145–179, doi: [10.1016/j.jvolgeores.2011.06.003](https://doi.org/10.1016/j.jvolgeores.2011.06.003)
- [12] D. J. Lowe, Tephrochronology and its application: A review, *Quaternary Geochronology* 6 (2011) 107–153, doi: [10.1016/j.quageo.2010.08.003](https://doi.org/10.1016/j.quageo.2010.08.003).
- [13] K. L. Wallace, M. I. Bursik, S. Kuehn, A. V. Kurbatov, P. Abbott, C. Bonadonna, K. Cashman, S. M. Davies, B. Jensen, C. Lane, G. Plunkett, V. C. Smith, E. Tomlinson, T. Thordarsson, and J. D. Walker, Community-

established best practice recommendations for tephra studies – from collection through analysis, Scientific Data 9 (2022) 447, doi: [10.1038/s41597-022-01515-y](https://doi.org/10.1038/s41597-022-01515-y).

[14] D. J. Lowe, N. J. G. Pearce, M. A. Jorgensen, S. C. Kuehn, C. A. Tryon, and C. L. Hayward, Correlating tephras and cryptotephras using glass compositional analyses and numerical and statistical methods: Review and evaluation, Quaternary Science Reviews 175 (2017) 1–44, doi: [10.1016/j.quascirev.2017.08.003](https://doi.org/10.1016/j.quascirev.2017.08.003).

[15] H. M. Innes, W. Hutchison, and A. Burke, Geochemical analysis of extremely fine-grained cryptotephra: New developments and recommended practices, Quaternary Geochronology 83 (2024) 101553, doi: [10.1016/j.quageo.2024.101553](https://doi.org/10.1016/j.quageo.2024.101553).

[16] Global Volcanism Program, Volcanoes of the World (v. 5.2.2), compiled by E. Venzke, distributed by Smithsonian Institution, 2024, <https://doi.org/10.5479/si.GVP.VOTW5-2024.5.2>

[17] H. Rawson, J. A. Naranjo, V. C. Smith, K. Fontijn, D. M. Pyle, T. A. Mather, and H. Moreno, The frequency and magnitude of post-glacial explosive eruptions at Volcán Mocho-Choshuencho, southern Chile, Journal of Volcanology and Geothermal Research 299 (2015) 103–129, doi: [10.1016/j.jvolgeores.2015.04.003](https://doi.org/10.1016/j.jvolgeores.2015.04.003).

[18] S. Bertrand, R. Daga, R. Bedert, and K. Fontijn, Deposition of the 2011–2012 Cordón Caulle tephra (Chile, 40°S) in lake sediments: Implications for tephrochronology and volcanology, Journal of Geophysical Research: Earth Surface 119 (2014) 2555–2573, doi: [10.1002/2014JF003321](https://doi.org/10.1002/2014JF003321).

[19] K. Mackay, M. R. Clark, S. Seabrook, E. Armstrong, N. Barr, G. Frontin-Rollet, S. George, L. Hoffmann, D. Macpherson, J. McInerney, S. Mills, R. Parsons-King, J. Roperez, E. Spain, R. Stewart, and O. Twigge, Environmental impacts of the 2022 eruption of Hunga Tonga – Hunga Ha'apai: voyage report of part 1 of the TESMaP survey of the region in April-May 2022 (TAN2206), NIWA Technical Report, 2022, 141, 197 p., <https://doi.org/10.13140/RG.2.2.24952.62727>

[20] G. Astuti, G. Giudice, D. Longo, C. D. Melita, G. Muscato, and A. Orlando, An Overview of the 'Volcan Project': An UAS for Exploration of Volcanic Environments, in: K. P. Valavanis, P. Oh, and L. A. Piegl (Eds.), Unmanned Aircraft Systems: International Symposium On Unmanned Aerial Vehicles, UAV'08, Dordrecht: Springer Netherlands, 2009, pp. 471–494. doi: [10.1007/978-1-4020-9137-7_25](https://doi.org/10.1007/978-1-4020-9137-7_25).

556 **References to the chapters of the 3rd edition of the Encyclopedia of Volcanoes [E1-E18]**

557 [E1] T. Ubide et al., Petrological characterisation of magma storage, in: C. Bonadonna et al. (Eds.), Part 1,
558 Chapter 4.2

559 [E2] C. Bonadonna et al. (Eds.), Part 3

560 [E3] L. Sandri et al., Volcanic hazard assessment, in: C. Bonadonna et al. (Eds.), Part 5, Chapter 2.1

561 [E4] J. Lindsay et al., Volcanic hazard maps, in: C. Bonadonna et al. (Eds.), Part 5, Chapter 2.2

562 [E5] N. Deligne et al., Qualitative and quantitative volcanic risk assesment, in: C. Bonadonna et al. (Eds.),
563 Part 5, Chapter 4.1

564 [E6] S. Barsotti et al., Syn-eruptive observations for primary volcanic hazard quantification, in: C.
565 Bonadonna et al. (Eds.), Part 6, Chapter 3.1

566 [E7] E. Joseph et al., Volcanic crises management, in: C. Bonadonna et al. (Eds.), Part 6, Chapter 3.2

567 [E8] M. Bebbington et al., Forecasting during eruption crises, in: C. Bonadonna et al. (Eds.), Part 6, Chapter
568 3.3

569 [E9] A. Jolley et al., Volcano education, in: C. Bonadonna et al. (Eds.), Part 7, Chapter 3.1

570 [E10] E. Calder et al., Engaging communities at risk: challenges and solutions, in: C. Bonadonna et al. (Eds.),
571 Part 7, Chapter 3.2

572 [E11] N. Fournier et al., Active volcanoes and tourism, in: C. Bonadonna et al. (Eds.), Part 7, Chapter 3.3

573 [E12] B. van Wyk de Vries et al., Volcano geoheritage – concepts, methods, community, resilience, in: C.
574 Bonadonna et al. (Eds.), Part 7, Chapter 3.4

575 [E13] S. Scott et al., Mining heat from geothermal systems in volcanic terrain, in: C. Bonadonna et al. (Eds.),
576 Part 8, Chapter 3.1

577 [E14] Y. Lavallee et al., Exploring and exploiting the magma-hydrothermal interface and super-critical
578 systems for heat and metals, in: C. Bonadonna et al. (Eds.), Part 8, Chapter 3.2

579 [E15] A. Simon et al., Formation and utilization of crustal magmatic ore deposits (porphyries, skarns and
580 pegmatites), in: C. Bonadonna et al. (Eds.), Part 8, Chapter 2.1

581 [E16] S. Tappe et al., Formation and utilization of ore-forming magmas from the mantle (kimberlites and
582 carbonatites), in: C. Bonadonna et al. (Eds.), Part 8, Chapter 2.2

583 [E17] L. Capra et al., Volcano flank instabilities and collapse, in : C. Bonnadonna et al. (Eds.), Part 3, Chapter
584 5.4

585 [E18] D. Pyle et al., Eruption size and classification, in: C. Bonadonna et al. (Eds.), Part 3, Chapter 2.7

586

587

588 Figures & Tables

589 **Figure 1:** Outcrop-scale photos of a range of volcanic rocks and deposits **(a)** Las Juntas andesite lava flow,
590 Tungurahua, Ecuador, showing cooling fractures at variable scales, including columnar jointing at the base; **(b)** Photo
591 of lava flows in the Southwest Rift Zone of Kīlauea, Hawai‘i, USA, demonstrating the principle of superposition, and
592 differences in weathering and vegetation based on their relative ages. The dark black lava flow erupted in 1823 CE;
593 it overlies the reddish-brown lava flow (bottom right), and both flows overlie an older lava flow (back right) that is
594 well vegetated with grass; **(c)** Valley-filling and sintered ignimbrite deposits, Valley of 10,000 Smokes, Alaska, USA;
595 **(d)** Angular unconformity in a sequence of pyroclastic fallout deposits at Totorillas, Chimborazo, Ecuador; **(e)**
596 Coherent andesitic lava flows (aeg) overlaying andesitic pyroclastic facies (ahc), adjacent to intrusive complex of
597 Hodge Crest at Prouty headwall, South Sister, Oregon, USA; **(f)** Rhyolite lava flow of Devils Chain (rdc), South Sister,
598 Oregon, USA. For unit abbreviations of photos **(e-f)** and sequence interpretations, see Case Study 1. All photos by
599 the authors.

600 **Figure 2 (How-To Box 1):** Summary overview of things to consider before going the field, including kit to take and
601 precautionary preparations

602 **Figure 3 (How-To Box 2):** Non-exhaustive overview of features to describe when mapping volcanic rocks and
603 deposits at a range of scales in the field, and some practical aspects to consider when sampling for different
604 purposes. Several features described in the field, such as sorting, modal abundance of components, or roundness of
605 clasts, are ideally estimated using visual comparison charts.

606 **Figure 4 (Case Study 1)** Simplified geologic map of South Sister, and its periphery, and several Middle Sister units, all
607 of which are part of the complete Three Sisters complex in Oregon, USA. North Sister is located ~7 km north of South
608 Sister. Colored geologic units are labeled with 3-letter unit designations; the first letter of each label indicates
609 composition: b=basalt; m=basaltic andesite (mafic units are shades of green and blue); d=dacite (pinks and purples);
610 a=andesite (oranges); r=rhyodacite and rhyolite (reds). For a full version of the Three Sisters volcanic cluster map,
611 including a legend and pamphlet with detailed unit descriptions and compositional and geochronological data, see
612 [\[11\]](#).

613 **Figure 5** Summary of explosive eruptions from Mocho-Choshuenco since the onset of deglaciation at ~18 ka. Each
614 of the 25 chemically and stratigraphically constrained units are represented by their modeled age probability
615 function, with the peak height scaled to the estimated eruption magnitude and color-coded by chemical
616 composition. Note that major Plinian eruptions are not evenly spaced in time, which is attributed to a response of
617 the magmatic plumbing systems to deglaciation. *Erosion rates, temperature, humidity and vegetation density*
618 *inferred from palaeoenvironmental reconstructions from a lake sediment core ca. 90 km South of Mocho-Choshuenco*
619 *(for references, see Additional Reading)*. Figure from [\[17\]](#).

620 **Figure 6** Orthomosaic (left, GSD 11.4 cm/px) and Digital Elevation Model with hillshade (right, GSD 23.4 cm/px) of
621 Cristal dome complex at Guagua Pichincha volcano, Ecuador. The red dashed lines correspond to the crater rims and
622 the blue dashed lines to the lava domes. The coordinate system is WGS 84, UTM zone 17S.

623 **Table 1.** Overview of key categories of volcanic rocks and deposits. For an exhaustive overview of classes of coherent
624 and volcanoclastic rocks and their essential characteristics, we refer to relevant chapters in this volume and [\[1\]](#).

625

626

627 **Additional Reading**

628 **[QR1]: Mapping volcano-related resources**

629 L. Cappelli, P. A. Wallace, A. Randazzo, P. M. Kamau, R. W. Njoroge, V. Otieno, M. S. Tubula, N. O. Mariita,
630 P. Mangi, and K. Fontijn, Diffuse soil CO₂ emissions at rift volcanoes: Structural controls and total budget
631 of the Olkaria Volcanic Complex (Kenya) case study, *Journal of Volcanology and Geothermal Research* 443
632 (2023) 107929, doi: [10.1016/j.jvolgeores.2023.107929](https://doi.org/10.1016/j.jvolgeores.2023.107929).

633 M. Chen, J. Wei, Y. Li, W. Shi, and N. Liu, Epithermal gold mineralization in Cretaceous volcanic belt, SE
634 China: Insight from the Shangshangang deposit, *Ore Geology Reviews* 118 (2020) 103355, doi:
635 [10.1016/j.oregeorev.2020.103355](https://doi.org/10.1016/j.oregeorev.2020.103355).

636 D. R. Cooke and S. F. Simmons, Characteristics and Genesis of Epithermal Gold Deposits, in: S. G.
637 Hagemann and P. E. Brown (Eds.), *Gold in 2000*, 13, Society of Economic Geologists, 2000, doi:
638 [10.5382/Rev.13.06](https://doi.org/10.5382/Rev.13.06).

639 A. Giuliani, M. W. Schmidt, T. H. Torsvik, and Y. Fedortchouk, Genesis and evolution of kimberlites, *Nature*
640 *Reviews Earth & Environment* 4 (2023) 738–753, doi: [10.1038/s43017-023-00481-2](https://doi.org/10.1038/s43017-023-00481-2).

641 E. Jolie, W. Hutchison, D. L. Driba, A. Jentsch, and B. Gizaw, Pinpointing Deep Geothermal Upflow in Zones
642 of Complex Tectono-Volcanic Degassing: New Insights from Aluto Volcano, Main Ethiopian Rift,
643 *Geochemistry Geophysics Geosystems* 20 (2019) 4146–4161, doi: [10.1029/2019GC008309](https://doi.org/10.1029/2019GC008309).

644 R. R. Large, J. McPhie, J. B. Gemmell, W. Herrmann, and G. J. Davidson, The Spectrum of Ore Deposit
645 Types, Volcanic Environments, Alteration Halos, and Related Exploration Vectors in Submarine Volcanic
646 Successions: Some Examples from Australia, *Economic Geology* 96 (2001) 913–938, doi:
647 [10.2113/gsecongeo.96.5.913](https://doi.org/10.2113/gsecongeo.96.5.913).

648 G. Norini, G. Gropelli, R. Sulpizio, G. Carrasco-Núñez, P. Dávila-Harris, C. Pelliccioli, F. Zucca, and R. De
649 Franco, Structural analysis and thermal remote sensing of the Los Humeros Volcanic Complex:
650 Implications for volcano structure and geothermal exploration, *Journal of Volcanology and Geothermal*
651 *Research* 301 (2015) 221–237, doi: [10.1016/j.jvolgeores.2015.05.014](https://doi.org/10.1016/j.jvolgeores.2015.05.014).

652 F. Rodríguez, N. M. Pérez, E. Padrón, G. Melián, P. Piña-Varas, S. Dionis, J. Barrancos, G. D. Padilla, P. A.
653 Hernández, R. Marrero, J. J. Ledo, F. Bellmunt, P. Queralt, A. Marcuello, and R. Hidalgo, Surface
654 geochemical and geophysical studies for geothermal exploration at the southern volcanic rift zone of
655 Tenerife, Canary Islands, Spain, *Geothermics* 55 (2015) 195–206, doi: [10.1016/j.geothermics.2015.02.007](https://doi.org/10.1016/j.geothermics.2015.02.007).

656 R. H. Sillitoe and H. F. Bonham, Volcanic landforms and ore deposits, *Economic Geology* 79 (1984) 1286–
657 1298, doi: [10.2113/gsecongeo.79.6.1286](https://doi.org/10.2113/gsecongeo.79.6.1286).

658 P. Stelling, L. Shevenell, N. Hinz, M. Coolbaugh, G. Melosh, and W. Cumming, Geothermal systems in
659 volcanic arcs: Volcanic characteristics and surface manifestations as indicators of geothermal potential
660 and favorability worldwide, *Journal of Volcanology and Geothermal Research* 324 (2016) 57–72, doi:
661 [10.1016/j.jvolgeores.2016.05.018](https://doi.org/10.1016/j.jvolgeores.2016.05.018).

662 J. Stix, B. Kennedy, M. Hannington, H. Gibson, R. Fiske, W. Mueller, and J. Franklin, Caldera-forming
663 processes and the origin of submarine volcanogenic massive sulfide deposits, *Geology* 31 (2003) 375–378,
664 doi: [10.1130/0091-7613\(2003\)031<0375:CFPATO>2.0.CO;2](https://doi.org/10.1130/0091-7613(2003)031<0375:CFPATO>2.0.CO;2).

665 F. Tornos, J. M. Peter, R. Allen, and C. Conde, Controls on the siting and style of volcanogenic massive
666 sulphide deposits, *Ore Geology Reviews* 68 (2015) 142–163, doi: [10.1016/j.oregeorev.2015.01.003](https://doi.org/10.1016/j.oregeorev.2015.01.003).

I. V. Vikentyev, E. V. Belogub, K. A. Novoselov, and V. P. Moloshag, Metamorphism of volcanogenic massive sulphide deposits in the Urals. *Ore geology, Ore Geology Reviews* 85 (2017) 30–63, doi: [10.1016/j.oregeorev.2016.10.032](https://doi.org/10.1016/j.oregeorev.2016.10.032).

[QR2]: Volcano-geological mapping and facies descriptions

G. Giordano, R. Cas, and J. V. Wright, The Geology of Volcanoes and Their Facies Models, in: R. Cas, G. Giordano, and J. V. Wright (Eds.), *Volcanology: Processes, Deposits, Geology and Resources*, Springer Textbooks in Earth Sciences, Geography and Environment, Springer International Publishing, 2024, pp. 1239–1426. doi: [10.1007/978-3-319-66613-6_16](https://doi.org/10.1007/978-3-319-66613-6_16).

J. V. Wright, G. Giordano, and R. Cas, Documenting the Geology of Volcanoes and Volcanic Terrains, in: R. Cas, G. Giordano, and J. V. Wright (Eds.), *Volcanology: Processes, Deposits, Geology and Resources*, Springer Textbooks in Earth Sciences, Geography and Environment, Springer International Publishing, 2024, pp. 1161–1236. doi: [10.1007/978-3-319-66613-6_15](https://doi.org/10.1007/978-3-319-66613-6_15).

E. M. A. Murphy and A. Salvador, International Stratigraphic Guide – an abridged version, *Episodes Journal of International Geoscience* 22 (1999) 255–271, <https://stratigraphy.org/guide/>.

R.V. Fisher, and H.-U. Schmincke, *Pyroclastic Rocks*, Springer-Verlag, 1984

D. Jerram, and N. Petford, The field description of igneous rocks, second edition, The geological field guide series, Wiley-Blackwell, 2011

R. J. Lisle, P. Brabham, and J. Barnes, Basic geological mapping, fifth edition, The geological field guide series, Wiley-Blackwell, 2011

F. Lucchi, C. A. Tranne, and P. L. Rossi, Stratigraphic approach to geological mapping of the late Quaternary volcanic island of Lipari (Aeolian archipelago, southern Italy), in: G. Groppe and L. Viereck-Goette (Eds.), *Stratigraphy and Geology of Volcanic Areas*, Geological Society of America, 2010, doi: [10.1130/2010.2464\(01\)](https://doi.org/10.1130/2010.2464(01)).

[QR3]: Collaborations

IAVCEI-INVOLC International Network for Volcanology Collaboration, Towards inclusive collaboration in volcanology: guidelines for best-engagement protocols in international collaboration, *Bulletin of Volcanology*, 86 (2024), 78, doi: [10.1007/s00445-024-01760-6](https://doi.org/10.1007/s00445-024-01760-6).

[QR4]: Chronology methods

D. E. Champion, D. T. Downs, M. E. Stelten, J. E. Robinson, T. W. Sisson, J. Shawali, K. Hassan, and H. M. Zahran, Paleomagnetism of the Harrat Rahat volcanic field, Kingdom of Saudi Arabia—Geologic unit correlations and geomagnetic cryptochron identifications, in: T. W. Sisson, A. T. Calvert, and W. D. Mooney (Eds.), *Active volcanism on the Arabian Shield—Geology, volcanology, and geophysics of northern Harrat Rahat and vicinity*, Kingdom of Saudi Arabia: U.S. Geological Survey Professional Paper 1862 (2023), 31 p., doi:[10.3133/pp1862H](https://doi.org/10.3133/pp1862H).

R. T. Holcomb, Eruptive history and long-term behavior of Kilauea volcano, in: R. W. Decker, T. L. Wright, and P. W. Stauffer, P.W. (Eds.), *Volcanism in Hawaii*: U.S. Geological Survey Professional Paper 1350 (1987) 261–350, <https://pubs.usgs.gov/pp/1987/1350/>.

707 A. J. Schaen, B. R. Jicha, K. V. Hodges, P. Vermeesch, M. E Stelten, C. M. Mercer, D. Phillips, T. A. Rivera, F.
708 Jourdan, E. L. Matchan, S. R. Hemming, L. E. Morgan, S. P. Kelley, W. S. Cassata, M. T. Heizler, P. M.
709 Vasconcelos, J. A. Benowitz, A. A. P. Koppers, D. F. Mark, E. M. Niespolo, C. J. Sprain, W. E. Hames, K. F.
710 Kuiper, B. D. Turrin, P. R. Renne, J. Ross, S. Nomade, H. Guillou, L. E. Webb, B. A. Cohen, A. T. Calvert, N.
711 Joyce, M. Ganerød, J. Wijbrans, O. Ishizuka, H. He, A. Ramirez, J. A. Pfänder, M. Lopez-Martínez, H. Qiu,
712 and B. S. Singer, Interpreting and reporting $^{40}\text{Ar}/^{39}\text{Ar}$ geochronologic data. Geological Society of America
713 Bulletin 133 (2020) 461–487, doi: <https://doi.org/10.1130/B35560.1>

714 L. Fedele, D. D. Insinga, A. T. Calvert, V. Morra, A. Perrotta, and C. Scarpati, $^{40}\text{Ar}/^{39}\text{Ar}$ dating of tuff vents
715 in the Campi Flegrei caldera (southern Italy): toward a new chronostratigraphic reconstruction of the
716 Holocene volcanic activity, Bulletin of Volcanology 73 (2011) 1323–1336, doi:
717 <https://doi.org/10.1007/s00445-011-0478-8>.

718 P. R. Renne, W. D. Sharp, A. L. Deino, G. Orsi, and L. Civetta, $^{40}\text{Ar}/^{39}\text{Ar}$ dating into the historical realm :
719 Calibration against Pliny the Younger, Science 277 (1997) 1279–1290, doi:
720 <https://doi.org/10.1126/science.277.5330.1279>.

721 J. L. Banner, Radiogenic isotopes: systematics and applications to earth surface processes and chemical
722 stratigraphy, Earth-Science Reviews 65 (2004) 141–194, [https://doi.org/10.1016/S0012-8252\(03\)00086-2](https://doi.org/10.1016/S0012-8252(03)00086-2).

723 M. Korte, M. C. Brown, S. R. Gunnarson, A. Nilsson, S. Panovska, I. Wardinski, and C. G. Constable, Refining
724 Holocene geochronologies using palaeomagnetic records, Quaternary Geochronology 50 (2019) 47–74,
725 <https://doi.org/10.1016/j.quageo.2018.11.004>.

726 T. J. Blackburn, D. F. Stockli, and J. D. Walker, Magnetite (U-Th)/He dating and its application to the
727 geochronology of intermediate to mafic volcanic rocks, Earth and Planetary Science Letters 259 (2007)
728 360–371, <https://doi.org/10.1016/j.epsl.2007.04.044>.

729 R. M. Flowers, P. K. Zeitler, M. Danišik, P. W. Reiners, C. Gautheron, R. A. Ketcham, J. R. Metcalf, D. F.
730 Stockli, E. Enkelmann, and R. W. Brown, (U-Th)/He chronology: Part 1. Data, uncertainty, and reporting,
731 Bulletin of the Geological Society of America 135 (2023) 104–136, <https://doi.org/10.1130/B36266.1>

732 P.-H. Blard, Cosmogenic ^3He in terrestrial rocks: A review, Chemical Geology 586 (2021) 120543,
733 <https://doi.org/10.1016/j.chemgeo.2021.120543>

734

735 **[QR5]: Magma plumbing systems, petrological monitoring**

736 C. Berthod, E. Médard, P. Bachèlery, L. Gurioli, A. Di Muro, A. Peltier, J.-C. Komorowski, M. Benbakkar, J.-
737 L. Devidal, J. Langlade, P. Besson, G. Boudon, E. Rose-Koga, C. Deplus, A. Le Friant, M. Bickert, S. Nowak,
738 I. Thion, P. Burckel, S. Hidalgo, M. Kaliwoda, S. J. Jorry, Y. Fouquet, and N. Feuillet, The 2018-ongoing
739 Mayotte submarine eruption: Magma migration imaged by petrological monitoring. Earth and Planetary
740 Science Letters 571 (2021) 117085. <https://doi.org/10.1016/j.epsl.2021.117085>

741 G. N. Fabbro, T. H. Druitt, and F. Costa, Storage and Eruption of Silicic Magma across the Transition from
742 Dominantly Effusive to Caldera-forming States at an Arc Volcano (Santorini, Greece), Journal of Petrology
743 58 (2017) 2429–2464, doi: [10.1093/petrology/egy013](https://doi.org/10.1093/petrology/egy013).

744 A. Harijoko, R. Uruma, H. E. Wibowo, L. D. Setijadji, A. Imai, K. Yonezu, and K. Watanabe, Geochronology
745 and magmatic evolution of the Dieng Volcanic Complex, Central Java, Indonesia and their relationships to
746 geothermal resources, Journal of Volcanology and Geothermal Research 310 (2016) 209–224, doi:
747 [10.1016/j.jvolgeores.2015.12.010](https://doi.org/10.1016/j.jvolgeores.2015.12.010).

O. Reubi, J. Blundy, and J. Pickles, Petrological Monitoring of Volcán de Colima Magmatic System: The 1998 to 2011 Activity, in: N. Varley, C. B. Connor, and J.-C. Komorowski (Eds.) Volcán de Colima: Portrait of a Persistently Hazardous Volcano, Berlin, Heidelberg: Springer Berlin Heidelberg, 2019, 219–240. doi: [10.1007/978-3-642-25911-1_9](https://doi.org/10.1007/978-3-642-25911-1_9).

F. Samrock, A. V. Grayver, O. Bachmann, Ö. Karakas, and M. O. Saar, Integrated magnetotelluric and petrological analysis of felsic magma reservoirs: Insights from Ethiopian rift volcanoes, Earth and Planetary Science Letters 559 (2021), 116765, doi: [10.1016/j.epsl.2021.116765](https://doi.org/10.1016/j.epsl.2021.116765).

K. Saunders, J. Blundy, R. Dohmen, and K. Cashman, Linking Petrology and Seismology at an Active Volcano, Science 336 (2012) 1023–1027, doi: [10.1126/science.1220066](https://doi.org/10.1126/science.1220066).

B. S. Singer, B. R. Jicha, M. A. Harper, J. A. Naranjo, L. E. Lara, and H. Moreno-Roa, Eruptive history, geochronology, and magmatic evolution of the Puyehue-Cordón Caulle volcanic complex, Chile, Bulletin of the Geological Society of America 120 (2008) 599–618, 2008, doi: [10.1130/B26276.1](https://doi.org/10.1130/B26276.1).

T. Yamamoto, T. Kudo, and O. Isizuka, Temporal variations in volumetric magma eruption rates of Quaternary volcanoes in Japan, Earth, Planets and Space 70 (2018), p. 65, doi: [10.1186/s40623-018-0849-x](https://doi.org/10.1186/s40623-018-0849-x).

A. G. Reyes, Petrology of Philippine geothermal systems and the application of alteration mineralogy to their assessment, Journal of Volcanology and Geothermal Research 43 (1990) 279–309, [https://doi.org/10.1016/0377-0273\(90\)90057-M](https://doi.org/10.1016/0377-0273(90)90057-M).

F. Lucci, G. Carrasco-Núñez, F. Rossetti, T. Theye, J. C. White, S. Urbani, H. Azizi, Y. Asahara, and G. Giordano, Anatomy of the magmatic plumbing system of Los Hornos Caldera (Mexico): implications for geothermal systems, Solid Earth 11 (2020) 125–159, <https://doi.org/10.5194/se-11-125-2020>.

[QR6]: Three Sisters, Oregon, USA

W. E. Scott, R. M. Iverson, S. P. Schilling, and B. J. Fisher, Volcano hazards in the Three Sisters region, Oregon (Report No. 99–437), Open-File Report (2001), <https://doi.org/10.3133/ofr99437>

D. Dzurisin, M. Lisowski, and C. W. Wicks, Continuing inflation at Three Sisters volcanic center, central Oregon Cascade Range, USA, from GPS, leveling, and InSAR observations, Bulletin of Volcanology 71 (2009) 1091–1110, doi: [10.1007/s00445-009-0296-4](https://doi.org/10.1007/s00445-009-0296-4).

A. T. Calvert, J. Fierstein, and W. Hildreth, Eruptive history of Middle Sister, Oregon Cascades, USA—Product of a late Pleistocene eruptive episode. Geosphere 14 (2018) 2118–2139. <https://doi.org/10.1130/GES01638.1>

D. F. Parker, J. D. Price, C. B. Brooks, and M. Ren, Contrasting magmatic evolutions of the Three Sister Volcanoes reflect increased heat flow, crustal melting and silicic magmatism in the Central Oregon Cascade Arc. Chemical Geology 618 (2023) 121294. <https://doi.org/10.1016/j.chemgeo.2022.121294>

[QR7]: Tephrostratigraphy and Tephrochronology: methods, databases and case studies

C. Martínez Fontaine, V. Peña-Araya, C. Marmo, M. Le Morvan, G. Delpech, K. Fontijn, G. Siani, and L. Cosyn-Westeen, BOOM! Tephrochronological dataset and exploration tool of the Southern (33–46° S) and Austral (49–55° S) volcanic zones of the Andes, Quaternary Science Reviews 316 (2023) 108254, <https://doi.org/10.1016/j.quascirev.2023.108254>.

788 S. P. E. Blockley, C. Bronk Ramsey, and D. M. Pyle, Improved age modelling and high-precision age
789 estimates of late Quaternary tephras, for accurate palaeoclimate reconstruction, *Journal of Volcanology*
790 and *Geothermal Research* 177 (2008) 251–262, doi: [10.1016/j.jvolgeores.2007.10.015](https://doi.org/10.1016/j.jvolgeores.2007.10.015).

791 C. Bronk Ramsey, Bayesian Analysis of Radiocarbon Dates, *Radiocarbon* 51 (2009) 337–360,
792 doi:10.1017/S0033822200033865

793 C. Bronk Ramsey, Dealing with Outliers and Offsets in Radiocarbon Dating, *Radiocarbon* 51 (2009) 1023–
794 1045, doi:10.1017/S0033822200034093

795 S. C. Kuehn, D. G. Froese, and P. A. R. Shane, The INTAV intercomparison of electron-beam microanalysis
796 of glass by tephrochronology laboratories: Results and recommendations, *Quaternary International* 246
797 (2011) 19–47, doi: [10.1016/j.quaint.2011.08.022](https://doi.org/10.1016/j.quaint.2011.08.022).

798 N. J. G. Pearce, W. T. Perkins, J. A. Westgate, and S. C. Wade, Trace-element microanalysis by LA-ICP-MS:
799 The quest for comprehensive chemical characterisation of single, sub-10 µm volcanic glass shards,
800 *Quaternary International* 246 (2011) 57–81, doi: [10.1016/j.quaint.2011.07.012](https://doi.org/10.1016/j.quaint.2011.07.012).

801 D. G. W. Smith and J. A. Westgate, Electron probe technique for characterising pyroclastic deposits, *Earth*
802 and *Planetary Science Letters* 5 (1968) 313–319, doi: [10.1016/S0012-821X\(68\)80058-5](https://doi.org/10.1016/S0012-821X(68)80058-5).

803 J. A. Westgate, W. T. Perkins, R. Fuge, N. J. G. Pearce, and A. G. Wintle, Trace-element analysis of volcanic
804 glass shards by laser ablation inductively coupled plasma mass spectrometry: application to
805 tephrochronological studies, *Applied Geochemistry* 9 (1994) 323–335, doi: [10.1016/0883-2927\(94\)90042-](https://doi.org/10.1016/0883-2927(94)90042-6)
806 [6](https://doi.org/10.1016/0883-2927(94)90042-6).

807 C. S. Feibel, Tephrostratigraphy and geological context in paleoanthropology, *Evolutionary Anthropology:*
808 *Issues, News, and Reviews* 8 (1999) 87–100. [https://doi.org/10.1002/\(SICI\)1520-6505\(1999\)8:3<87::AID-](https://doi.org/10.1002/(SICI)1520-6505(1999)8:3<87::AID-EVAN4>3.0.CO;2-W)
809 [EVAN4>3.0.CO;2-W](https://doi.org/10.1002/(SICI)1520-6505(1999)8:3<87::AID-EVAN4>3.0.CO;2-W)

810 S. M. Davies, P. G. Albert, A. J. Bourne, S. Owen, A. Svensson, M. S. M. Bolton, E. Cook, B. J. L. Jensen, G.
811 Jones, V. V. Ponomareva, and T. Suzuki, Exploiting the Greenland volcanic ash repository to date caldera-
812 forming eruptions and widespread isochrons during the Holocene, *Quaternary Science Reviews* 334
813 (2024) 108707. <https://doi.org/10.1016/j.quascirev.2024.108707>

814 A. J. Bourne, P. M. Abbott, P. G. Albert, E. Cook, N. J. G. Pearce, V. Ponomareva, A. Svensson, and S. M.
815 Davies, Underestimated risks of recurrent long-range ash dispersal from northern Pacific Arc volcanoes,
816 *Scientific Reports* 6 (2016) 29837. <https://doi.org/10.1038/srep29837>

817 V. Ponomareva, M. Portnyagin, and S. M. Davies, Tephra without Borders: Far-Reaching Clues into Past
818 Explosive Eruptions, *Frontiers in Earth Science* 3 (2015). <https://doi.org/10.3389/feart.2015.00083>

819 K. V. Cashman, and A. C. Rust, Far-travelled ash in past and future eruptions: combining tephrochronology
820 with volcanic studies, *Journal of Quaternary Science* 35 (2020) 11–22. <https://doi.org/10.1002/jqs.3159>

821 C. Bronk Ramsey, R. A. Housley, C. S. Lane, V. C. Smith, and A. M. Pollard, The RESET tephra database and
822 associated analytical tools, *Quaternary Science Reviews* 118 (2015) 33–47.
823 <https://doi.org/10.1016/j.quascirev.2014.11.008>

824 K. Fontijn, K. McNamara, A. Z. Tadesse, D. M. Pyle, F. Dessalegn, W. Hutchison, T. A. Mather, and G. Yirgu,
825 Contrasting styles of post-caldera volcanism along the Main Ethiopian Rift: Implications for contemporary
826 volcanic hazards, *Journal of Volcanology and Geothermal Research* 356 (2018) 90–113, doi:
827 [10.1016/j.jvolgeores.2018.02.001](https://doi.org/10.1016/j.jvolgeores.2018.02.001).

828 M. Marcaida, J. A. Vazquez, M. E. Stelten, and J. S. Miller, Constraining the Early Eruptive History of the
 829 Mono Craters Rhyolites, California, Based on ^{238}U - ^{230}Th Isochron Dating of Their Explosive and Effusive
 830 Products, *Geochemistry, Geophysics, Geosystems* 20 (2019) 1539–1556, doi: [10.1029/2018GC008052](https://doi.org/10.1029/2018GC008052).

831 N. W. Dunbar, and A. V. Kurbatov, Tephrochronology of the Siple Dome ice core, West Antarctica:
 832 correlations and sources, *Quaternary Science Reviews* 30 (2011) 1602–1614.
 833 <https://doi.org/10.1016/j.quascirev.2011.03.015>

834 N. J. G. Pearce, P. M. Abbott, and C. Martin-Jones, Microbeam methods for the analysis of glass in fine-
 835 grained tephra deposits: A SMART perspective on current and future trends, *Geological Society Special*
 836 *Publication* 398 (2014) 29–46. <https://doi.org/10.1144/SP398.1>

837 P. A. Wallace, V. Otieno, P. Godec, R. W. Njoroge, M. S. Tubula, L. Cappelli, P. M. Kamau, S. Nomade, N. O.
 838 Mariita, and K. Fontijn, Temporal and spatial evolution of explosive silicic peralkaline eruptions at the
 839 Olkaria Volcanic Complex and Longonot volcano in the Southern Kenya Rift, *Journal of Volcanology and*
 840 *Geothermal Research* (2025), 108275, <https://doi.org/10.1016/j.jvolgeores.2025.108275>.

841

842 **[QR8]: Southern and Austral Volcanic Zone, Chile**

843 K. Fontijn, S. M. Lachowycz, H. Rawson, D. M. Pyle, T. A. Mather, J. A. Naranjo, and H. Moreno, Late
 844 Quaternary tephrostratigraphy of southern Chile and Argentina, *Quaternary Science Reviews* 89 (2014)
 845 70–84, doi: [10.1016/j.quascirev.2014.02.007](https://doi.org/10.1016/j.quascirev.2014.02.007).

846 K. Fontijn, H. Rawson, M. Van Daele, J. Moernaut, A. M. Abarzúa, K. Heirman, S. Bertrand, D. M. Pyle, T.
 847 A. Mather, M. De Batist, J. A. Naranjo, and H. Moreno, Synchronisation of sedimentary records using
 848 tephra: A postglacial tephrochronological model for the Chilean Lake District, *Quaternary Science Reviews*
 849 137 (2016) 234–254, doi: [10.1016/j.quascirev.2016.02.015](https://doi.org/10.1016/j.quascirev.2016.02.015).

850 M. R. Kaplan, C. J. Fogwill, D. E. Sugden, N. R. J. Hulton, P. W. Kubik, and S. P. H. T. Freeman, Southern
 851 Patagonian glacial chronology for the Last Glacial period and implications for Southern Ocean climate,
 852 *Quaternary Science Reviews* 27 (2008) 284–294, doi: [10.1016/j.quascirev.2007.09.013](https://doi.org/10.1016/j.quascirev.2007.09.013).

853 R. E. Smith, V. C. Smith, K. Fontijn, A. C. Gebhardt, S. Wastegård, B. Zolitschka, C. Ohlendorf, C. Stern, and
 854 C. Mayr, Refining the Late Quaternary tephrochronology for southern South America using the Laguna
 855 Potrok Aike sedimentary record, *Quaternary Science Reviews* 218 (2019) 137–156, doi:
 856 [10.1016/j.quascirev.2019.06.001](https://doi.org/10.1016/j.quascirev.2019.06.001).

857 J. Moernaut, M. Van Daele, K. Heirman, K. Fontijn, M. Strasser, M. Pino, R. Urrutia, and M. De Batist,
 858 Lacustrine turbidites as a tool for quantitative earthquake reconstruction: New evidence for a variable
 859 rupture mode in south central Chile, *Journal of Geophysical Research: Solid Earth* 119 (2014) 1607–1633.
 860 <https://doi.org/10.1002/2013JB010738>

861 S. F. L. Watt, D. M. Pyle, and T. A. Mather, Evidence of mid- to late-Holocene explosive rhyolitic eruptions
 862 from Chaitén Volcano, Chile, *Andean Geology* 40 (2013) 216–226. [https://doi.org/10.5027/andgeoV40n2-](https://doi.org/10.5027/andgeoV40n2-a02)
 863 [a02](https://doi.org/10.5027/andgeoV40n2-a02)

864 S. F. L. Watt, D. M. Pyle, J. A. Naranjo, G. Rosqvist, M. Mella, T. A. Mather, and H. Moreno, Holocene
 865 tephrochronology of the Hualaihue region (Andean southern volcanic zone, $\sim 42^\circ\text{S}$), southern Chile,
 866 *Quaternary International* 246 (2011) 324–343. <https://doi.org/10.1016/j.quaint.2011.05.029>

867 D. J. Weller, C. G. Miranda, P. I. Moreno, R. Villa-Martínez, and C. R. Stern, Tephrochronology of the
 868 southernmost Andean Southern Volcanic Zone, Chile, *Bulletin of Volcanology* 77 (2015) 1–24.
 869 <https://doi.org/10.1007/s00445-015-0991-2>

M. Van Daele, J. Moernaut, G. Silversmit, S. Schmidt, K. Fontijn, K. Heirman, W. Vandoorne, M. De Clercq, J. Van Acker, C. Wolff, M. Pino, R. Urrutia, S. J. Roberts, L. Vincze, and M. De Batist, The 600 yr eruptive history of Villarrica Volcano (Chile) revealed by annually laminated lake sediments, *Bulletin of the Geological Society of America* 126 (2014) 481–498. <https://doi.org/10.1130/B30798.1>

B. Klaes, G. Wörner, K. Kremer, K. Simon, A. Kronz, D. Scholz, C. W. Mueller, C. Höschen, J. Struck, H. W. Arz, S. Thiele-Bruhn, D. Schimpf, and R. Kilian, High-resolution stalagmite stratigraphy supports the Late Holocene tephrochronology of southernmost Patagonia, *Communications Earth & Environment* 3 (2022) 23. <https://doi.org/10.1038/s43247-022-00358-0>

D. Weller, M. de Porras, A. Maldonado, C. Méndez, and C. Stern, New age controls on the tephrochronology of the southernmost Andean Southern Volcanic Zone, Chile, *Quaternary Research* 91 (2019) 250–264, <https://doi.org/10.1017/qua.2018.81>

S. Bertrand, F. Charlet, B. Charlier, V. Renson, N. Fagel, N. Climate variability of southern Chile since the Last Glacial Maximum: a continuous sedimentological record from Lago Puyehue (40°S), *Journal of Paleolimnology* 39 (2008) 179–195. <https://doi.org/10.1007/s10933-007-9117-y>

L. Vargas-Ramirez, E. Roche, P. Gerrienne, H. Hooghiemstra, A pollen-based record of late glacial–Holocene climatic variability in the southern lake district, Chile, *Journal of Paleolimnology* 39 (2008) 197–217. <https://doi.org/10.1007/s10933-007-9115-0>

[QR9]: Modern eruptions

C. Bonadonna, R. Cioni, M. Pistolesi, M. Elissondo, and V. Baumann, Sedimentation of long-lasting wind-affected volcanic plumes: the example of the 2011 rhyolitic Cordón Caulle eruption, Chile, *Bulletin of Volcanology* 77 (2015), 13, doi: [10.1007/s00445-015-0900-8](https://doi.org/10.1007/s00445-015-0900-8).

P. Forte, L. Domínguez, C. Bonadonna, C. E. Gregg, D. Bran, D. Bird, and J. M. Castro, Ash resuspension related to the 2011–2012 Cordón Caulle eruption, Chile, in a rural community of Patagonia, Argentina, *Journal of Volcanology and Geothermal Research* 350 (2018) 18–32, doi: [10.1016/j.jvolgeores.2017.11.021](https://doi.org/10.1016/j.jvolgeores.2017.11.021).

M. Pistolesi, R. Cioni, C. Bonadonna, M. Elissondo, V. Baumann, A. Bertagini, L. Chiari, R. Gonzales, M. Rosi, and L. Francalanci, Complex dynamics of small-moderate volcanic events: the example of the 2011 rhyolitic Cordón Caulle eruption, Chile, *Bulletin of Volcanology* 77 (2015) 3, doi: [10.1007/s00445-014-0898-3](https://doi.org/10.1007/s00445-014-0898-3).

G. B. M. Pedersen, J. M. C. Belart, B. V. Óskarsson, M. T. Gudmundsson, N. Gies, T. Högnadóttir, Á. R. Hjartardóttir, V. Pinel, E. Berthier, T. Dürig, H. I. Reynolds, C. W. Hamilton, G. Valsson, P. Einarsson, D. Ben-Yehosua, A. Gunnarsson, and B. Oddsson, Volume, Effusion Rate, and Lava Transport During the 2021 Fagradalsfjall Eruption: Results From Near Real-Time Photogrammetric Monitoring, *Geophysical Research Letters* 49 (2022) e2021GL097125. <https://doi.org/10.1029/2021GL097125>

Á. R. Hjartardóttir, T. Dürig, M. Parks, V. Drouin, V. Eyjólfsson, H. Reynolds, P. Einarsson, E. H. Jensen, B. V. Óskarsson, J. M. C. Belart, J. Ruch, N. B. Gies, and G. B. M. Pedersen, Pre-existing fractures and eruptive vent openings during the 2021 Fagradalsfjall eruption, Iceland, *Bulletin of Volcanology* 85 (2023) 56. <https://doi.org/10.1007/s00445-023-01670-z>

C. Ducrocq, T. Árnadóttir, P. Einarsson, S. Jónsson, V. Drouin, H. Geirsson, and Á. R. Hjartardóttir, Widespread fracture movements during a volcano-tectonic unrest: the Reykjanes Peninsula, Iceland, from

911 2019–2021 TerraSAR-X interferometry, Bulletin of Volcanology 86 (2024) 14.
912 <https://doi.org/10.1007/s00445-023-01699-0>

913 A. K. Gupta, R. Bennartz, K. E. Fauria, and T. Mittal, Eruption chronology of the December 2021 to January
914 2022 Hunga Tonga-Hunga Ha’apai eruption sequence, Communications Earth & Environment 3 (2022)
915 314. <https://doi.org/10.1038/s43247-022-00606-3>

916

917 **[QR10]: Recent advances**

918 S. D. Andrade, E. Saltos, V. Nogales, S. Cruz, G. Lee, and J. Barclay, Detailed Cartography of Cotopaxi’s 1877
919 Primary Lahar Deposits Obtained by Drone-Imagery and Field Surveys in the Proximal Northern Drainage,
920 Remote Sensing 14 (2022) 3, doi: [10.3390/rs14030631](https://doi.org/10.3390/rs14030631).

921 H. Darmawan, T. R. Walter, K. S. Brotopuspito, Subandriyo, and I Gusti Made Agung Nandaka,
922 Morphological and structural changes at the Merapi lava dome monitored in 2012–15 using unmanned
923 aerial vehicles (UAVs), Journal of Volcanology and Geothermal Research 349 (2018) 256–267, doi:
924 [10.1016/j.jvolgeores.2017.11.006](https://doi.org/10.1016/j.jvolgeores.2017.11.006).

925 M. Favalli, A. Fornaciai, L. Nannipieri, A. Harris, S. Calvari, and C. Lormand, UAV-based remote sensing
926 surveys of lava flow fields: a case study from Etna’s 1974 channel-fed lava flows, Bulletin of Volcanology
927 80 (2018), 29, doi: [10.1007/s00445-018-1192-6](https://doi.org/10.1007/s00445-018-1192-6).

928 T. Nakano, I. Kamiya, M. Tobita, J. Iwahashi, and H. Nakajima, Landform monitoring in active volcano by
929 UAV and SfM-MVS technique, The International Archives of the Photogrammetry, Remote Sensing and
930 Spatial Information Sciences, XL–8 (2014) 71–75, doi: [10.5194/isprsarchives-XL-8-71-2014](https://doi.org/10.5194/isprsarchives-XL-8-71-2014).

931 A. Román, A. Tovar-Sánchez, D. Roque-Atienza, I. E. Huertas, I. Caballero, E. Fraile-Nuez, and G. Navarro,
932 Unmanned aerial vehicles (UAVs) as a tool for hazard assessment: The 2021 eruption of Cumbre Vieja
933 volcano, La Palma Island (Spain), Science of The Total Environment 843 (2022) 157092, doi:
934 [10.1016/j.scitotenv.2022.157092](https://doi.org/10.1016/j.scitotenv.2022.157092).

935 A. V. Shevchenko, V. N. Dvigalo, T. R. Walter, R. Mania, F. Maccaferri, I. Y. Svirid, A. B. Belousov, and M. G.
936 Belousova, The rebirth and evolution of Bezymianny volcano, Kamchatka after the 1956 sector collapse,
937 Communications Earth & Environment 1 (2020), 15, doi: [10.1038/s43247-020-00014-5](https://doi.org/10.1038/s43247-020-00014-5).

938

939